AAS 23-022

MOMENTUM UNLOAD MANEUVER PLANNING FOR A LUNAR NAVIGATION SATELLITE

Mark Hartigan*, Noble Hatten†, and Sun Hur-Diaz†

NASA is "developing" an infrastructure at the Moon called LunaNet to provide position, navigation, and timing (PNT) services to orbiting and surface users on the Moon. One reference orbit that has been considered for a Lunar Navigation Node (LNN) is a 12-hour frozen orbit. The impact of regularly scheduled momentum unload maneuvers on such an orbit and its PNT service availability was analyzed, and an approach was established to minimize their disturbances to the orbit. Goddard's General Mission Analysis Tool (GMAT) was used to survey the effects of momentum unload maneuver timing and direction on orbit stability and find an appropriate solution. For a LNN satellite autonomously performing its orbit determination (OD), the impact of timing and direction of the momentum unloads on PNT service availability was analyzed using a combination of Monte-Carlo techniques and linear covariance analysis with Goddard's Orbit Determination Toolbox (ODTBX). For the reference frozen orbit, performing momentum unloads near apoapsis and in the orbit-normal direction was found to strike the best balance between service availability and orbit perturbation. Adopting this approach will improve service uptime of the LNN by reducing outages from momentum unloads, as well as save fuel and extend mission life by minimizing the need for corrective maneuvers.

INTRODUCTION

Recent years have brought a growing interest in establishing a presence in cislunar space as technology has matured and research interests have turned towards unexplored areas of the Moon. Prominent among recent plans is NASA's Artemis program to establish a sustainable human presence on the lunar surface and in cislunar space. Maintaining this human presence will require unprecedented communications, navigation, and networking capabilities: enter LunaNet, an architecture specification developed by NASA's Space Communications and Navigation program to rapidly develop these capabilities at the Moon.[1,2]

The LunaNet architecture includes a constellation of relay satellites that will allow communication between the lunar surface and Earth, as well as provide a position, navigation, and timing (PNT) service to users on the lunar surface and in orbit – initial plans target the lunar South Pole as an area of scientific interest. These relay satellites are also referred to as Lunar Navigation Nodes (LNN).

A candidate orbit for the LNN is an elliptical lunar frozen orbit with a semi-major axis ~ 6000 km and a period of 12 hours, shown in Figure 1.[3] In this configuration of orbital elements (Table 1), the satellite orbit can be kept stable by third (Earth) and fourth (Sun) body perturbations if certain conditions are met. These conditions are outlined by Ely and the corresponding orbits are referred

*Graduate Research Assistant, Department of Aerospace Engineering, Georgia Institute of Technology, Atlanta, GA. hartigan@gatech.edu

†Aerospace engineer, Navigation and Mission Design Branch, NASA Goddard Space Flight Center, Greenbelt, MD.

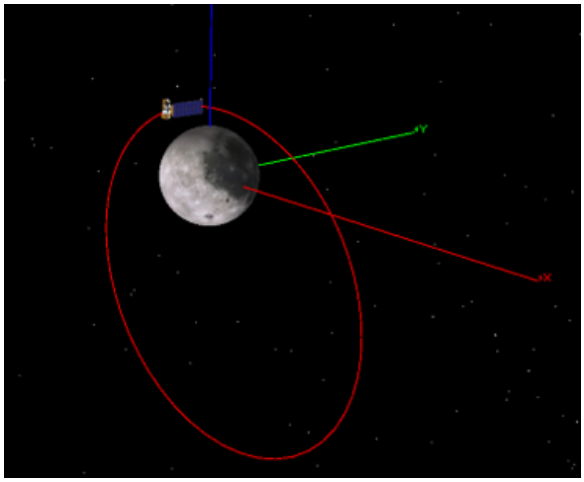

Figure 1: Graphical depiction of a sample LNN satellite orbit about the Moon.

to as lunar frozen orbits.[4] Using a lunar frozen orbit helps to minimize station-keeping maneuver requirements for the mission as the spacecraft can passively maintain its orbit. However, torques from external sources such as solar radiation pressure combined with internal sources like antenna pointing requirements mean that reaction wheels will need to be desaturated regularly in order to maintain attitude control authority. Depending on thruster configuration, thruster misalignments, and center of mass knowledge, performing these regularly scheduled momentum unloads can result in a residual translational velocity.

Strategies for addressing this relatively common issue vary widely based on mission requirements and target orbital regime. One common approach is to solve a simplified model analytically then verify with numerical analysis.[5] More complex techniques have also been developed such as using Model Predictive Control to minimize Δv expenditure[6] or formulating it as a reinforcement learning problem.[7] For this paper, a combination of analytic and numerical analyses is chosen. This is due to the complexity and computational intensity of performing the navigation analysis to determine impacts on service availability.

Users of the LNN PNT service derive their state estimate from the provider satellites' own OD – which, unlike GPS, isn't provided by a ground segment. Rather, each LNN satellite will perform its own OD. In this paper, we consider OD using a combination of weak-signal Global Navigation Satellite Systems (GNSS) and optical navigation (OpNav) ranging to the Moon.[8] Depending on the thruster geometry, momentum unloads can result in residual Δv that can negatively impact both the orbit stability and the satellite OD knowledge, the former of which could necessitate an additional maneuver to maintain orbital requirements, and the latter of which may cause a PNT service outage if the mission requirements for maximum OD uncertainty are violated. This paper provides a detailed analysis of resulting orbit stability based on maneuver location and direction, followed by a similar analysis from the navigation perspective. A recommendation specific to the reference frozen orbit is generated, but results provide more general insight into the effects of Δv maneuvers on lunar frozen orbit stability and satellite navigation uncertainty.

ORBIT STABILITY

Orbit stability performance after a maneuver is based on the goal of maintaining the frozen orbit. A sensitivity analysis was conducted using maneuver location and direction as the independent variables. Periapsis, apoapsis, and the descending node were chosen as locations of interest, with the ascending node not included for brevity and its similarity with the descending node. The velocity, orbit-normal, and binormal directions (Figure 2) were chosen primarily because of these directions' relevance to efficiency in changing various orbital parameters. In principle, a maneuver in the velocity direction is most efficient for performing an orbit-raising maneuver.

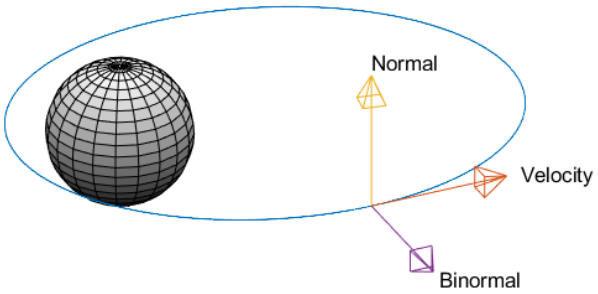

Figure 2: The Velocity-Normal-Binormal (VNB) frame.

Maneuver-Free Case

Lunar orbits with specific values of inclination, i, eccentricity, e, semi-major axis, a, and argument of periapsis, ω, such as the set tabulated in Table 1 can lead to stable orbits where the drift of orbital parameters is mitigated or eliminated completely.[4] Ely solved the orbit disturbing function R given in Equation (1) using Lagrange's planetary equations to solutions where generally $\frac{de}{dt} = \frac{d\omega}{dt} = 0$ for long period oscillations.

$$R = \frac{\gamma n^2 a^2}{16\sqrt{1-e^2}}[(1+3\cos 2i)(1+\frac{3}{2}e^2) + 15e^2 \sin^2 i \cos 2\omega] \tag{1}$$

Figure 3 plots orbital elements for a 12-hour frozen orbit over one year, with the spacecraft conducting no maneuvers. For these propagations, the modeled dynamics include non-spherical gravity of the Moon up to degree and order 64 and point mass gravity of the Sun and every planet in the solar system. Planetary ephemerides were obtained by GMAT using NAIF SPICE.[9–11] To analyze the impact of maneuvers on the stability of these orbits, the behavior of e versus ω can be observed. Since a lunar frozen orbit is considered, the long-period oscillations of this plot (Figure 3a) roughly form a closed circle, indicating it repeats. Generally, observing how well the data forms a small, closed circle on this plot is a strong indicator of stability. Periapsis is plotted on the right (Figure 3b) to check for surface impaction and adherence to the maneuver-free case.

Table 1: Orbital elements of lunar frozen orbit (Moon Principal Axis – Inertial at J2000).

Orbital Element	Value
Initial epoch	27 May 2024, 12:16:34
Semi-major axis, a	6142 km
Eccentricity, e	0.57
Inclination, i	57°
RAAN, Ω	100.8°
AOP, ω	90°
True anomaly, θ_0	0°

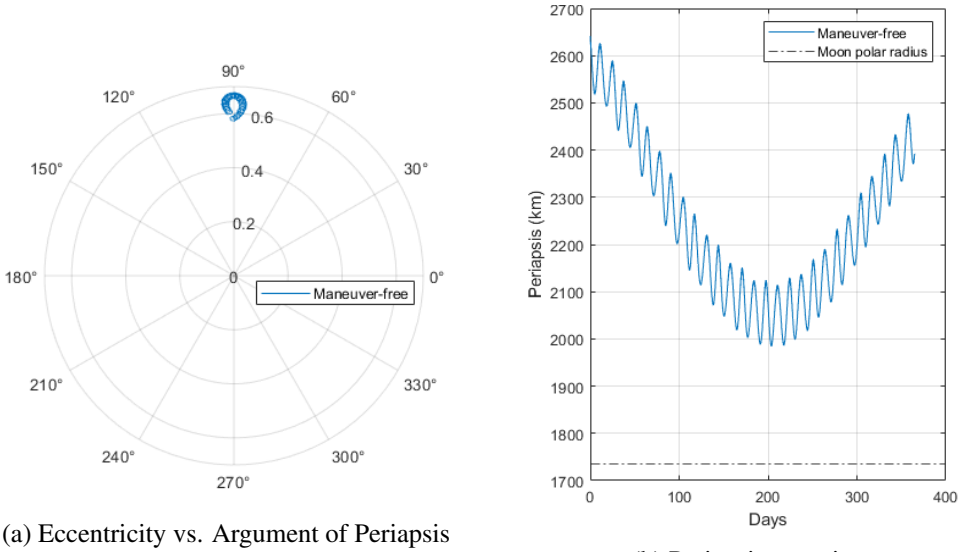

(a) Eccentricity vs. Argument of Periapsis

(b) Periapsis over time

Figure 3: Orbital elements (OE) over one year in a lunar frozen orbit.

Maneuver Impacts

To emphasize the effects of maneuvers on orbit stability, a 100-m/s Δv is first performed and overlaid on the maneuver-free data in Figures 4 and 5. This Δv is much larger than a momentum unload but is helpful for visualizing the different effects produced by maneuvers in different directions. In these propagations and throughout the paper, Δv maneuvers are modelled as impulsive. Figure 4 shows the resulting orbital elements for the first year after performing the maneuver in the velocity direction at the descending node. This is an example of a poor direction for maintaining orbit stability; the velocity direction is optimal for performing coplanar orbit changes, resulting in large changes to semimajor axis and eccentricity. This is obviously undesirable for minimizing changes to eccentricity. The descending node proves to be a suboptimal location as well; the goal of this exercise is to minimize changes in both magnitude and direction of the velocity vector pre- and post-maneuver, so it logically follows that starting with the largest velocity magnitude (i.e., at periapsis) will minimize the relative change in vector magnitude, regardless of maneuver direction. The binormal direction is also suboptimal, as it drastically shifts argument of periapsis by several

degrees.

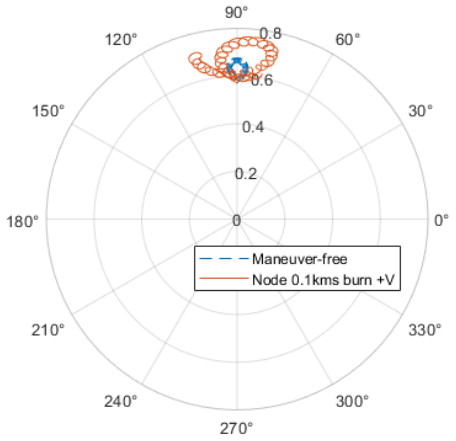

(a) Eccentricity vs. Argument of Periapsis

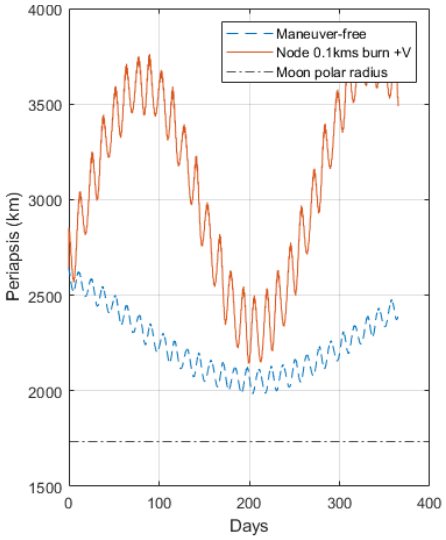

(b) Periapsis over time

Figure 4: OE over one year after a 100 m/s burn in the velocity direction at the descending node.

What remains is performing the momentum unload maneuver at periapsis with the residual in the orbit-normal direction, the results of which can be seen in Figure 5. Firing in the orbit-normal direction at periapsis primarily changes the right ascension of the ascending node, but rather inefficiently, so it adheres to the unperturbed case the best of any of these large maneuvers.

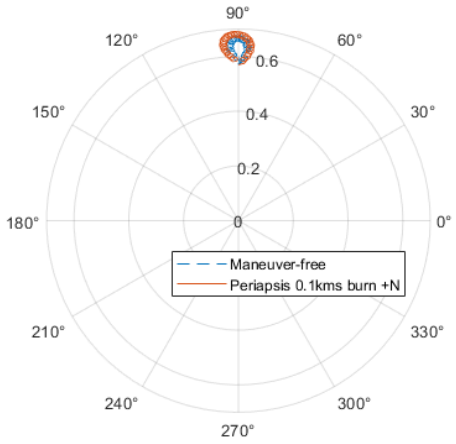

(a) Eccentricity vs. Argument of Periapsis

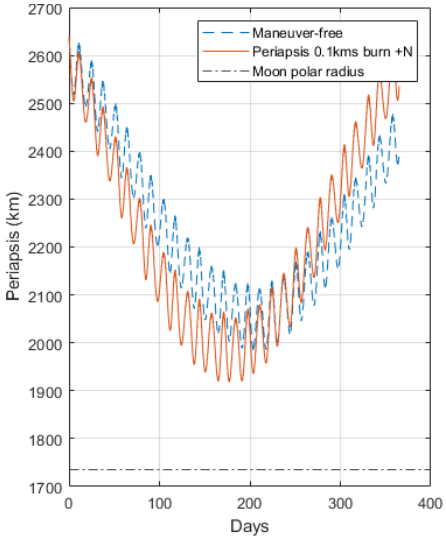

(b) Periapsis over time

Figure 5: OE over one year after a 100 m/s burn in the orbit-normal direction at periapsis.

For a sample thruster configuration and bus design of a LNN, we assume regular momentum

unload maneuvers impart a Δv residual on the order of 10 cm/s at a cadence of once every two weeks. In Figure 6, the results of a momentum unload scenario with these parameters are shown. The momentum unloads are aligned so the residual is along the orbit-normal direction at periapsis. Maneuvers are alternated between the positive and negative directions, which effectively stops any drift of orbital elements caused by the previous maneuver. This permits the satellite to maintain its natural orbit stability while performing these momentum unload maneuvers. While applying this scheme at other orbit locations and in other maneuver directions would help adhere to the stability criteria as well, they still drift more than the normal direction at periapsis and would thus require more stationkeeping maneuvers in the long run.

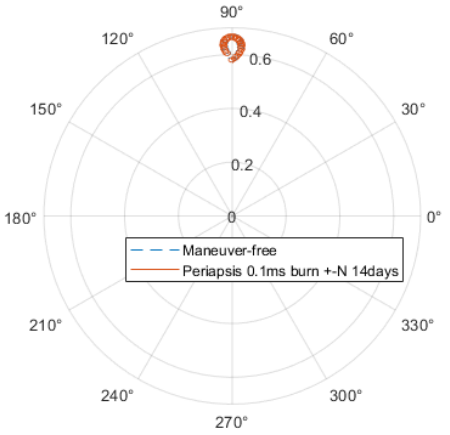

(a) Eccentricity vs. Argument of Periapsis

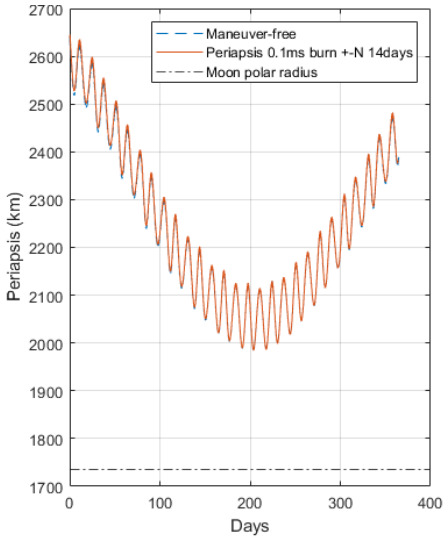

(b) Periapsis over time

Figure 6: OE over one year with 10 cm/s burns every 14 days along the orbit-normal axis at periapsis, alternating positive and negative directions.

NAVIGATION ANALYSIS

Maneuvers negatively impact the satellite OD accuracy for a period after the maneuver occurs due to errors in the executed maneuver magnitude and direction which get propagated by the model and need to be compensated for by adding additional uncertainty to the navigation solution.[12] Since the impact of these maneuver errors on the model dynamics (and therefore navigation accuracy) will change based on placement within the orbit, finding the best direction and location to perform a maneuver to maximize service availability is critical to the mission.

Analysis Setup

Orbit Determination Toolbox (ODTBX)* is a MATLAB toolbox developed by NASA Goddard Space Flight Center (GSFC) for early-mission-phase navigation analysis.[13] ODTBX is a generalized and well-featured tool, but in this study, it is primarily used for Monte-Carlo simulations, linear

*https://opensource.gsfc.nasa.gov/projects/ODTBX/

covariance analysis, and measurement processing. Using this tool, an approximation of LNN navigation can be established and covariance analysis performed. To reduce computational complexity, navigation measurements and processing are simplified. The primary purpose of this analysis is to compare relative changes in navigation performance between maneuvers – analysis using more realistic models has also been performed by GSFC to assess the performance of a system of lunar relay satellites.[3] However, the impacts of stationkeeping maneuvers on navigation performance were not evaluated in that paper.

For the simplification, we assume navigation based on weak-signal GNSS and OpNav ranging to the Moon, with the OD resolved using an extended Kalman filter (EKF).[14] Weak-signal GNSS and OpNav measurements were approximated as ranging to the Earth and Moon, respectively, as shown in Equations (2) and (3) – the satellite's current position given as r and $h(r,t)$ is the measurement range at a given position and time.

$$h_{GNSS}(r,t) = ||r(t) - r_{Earth}(t)||_2 \tag{2}$$

$$h_{OpNav}(r,t) = ||r(t) - r_{Moon}(t)||_2 \tag{3}$$

The measurement noise covariance was assumed to be constant for weak GNSS, since the changes in satellite position relative to the Earth are small compared to the Earth-Moon distance. Measurement noise covariance for OpNav was scaled with the square of satellite altitude above the lunar surface because the spacecraft's optical navigation is based on shape recognition of the Moon. The baselined accelerometer for this mission has a resolution of 3 mm/s^2, and the error introduced by each maneuver is assumed to have a standard deviation of half the resolution multiplied by a 1-second duration of the maneuver – this equals a 1σ error of 1.5 mm/s applied to the 10 cm/s momentum unload. This error was applied in all 3 axes, as would be output from a 3-axis accelerometer. The residual Δv from each momentum unload was directed in the orbit normal direction, as this is considered to be the least detrimental to orbit stability (as discussed in previous sections).

Each simulation was propagated for 48 hours, or 4 orbits, to allow the navigation filter to converge to steady state. A maneuver is performed at this point. Then, the simulation is propagated for another 48 hours to allow the filter to return to steady state. To aid this process, the EKF was adjusted by increasing the process noise for a finite amount of time post-maneuver. The process noise power spectral density matrix in the EKF to capture the maneuver uncertainty can be modeled as

$$Q(t) = \begin{bmatrix} 0_{3\times3} & & 0_{3\times3} & \\ & 10^{-9} & 0 & 0 \\ 0_{3\times3} & 0 & 10^{-9} & 0 \\ & 0 & 0 & 10^{-9} \end{bmatrix} * Q_{scale}(t) \tag{4}$$

Q_{scale} is generally constant but is increased for a period of time, τ_{scale}, after the maneuver as listed in Table 2. The values in the table were computed to minimize the reconvergence time after the maneuver perturbation.

Maneuver-Free Case

Figure 7 is a plot of the root-sum-of-squares (RSS) position error in the unperturbed case in which the navigation filter is propagated – beginning at periapsis – for 96 hours without maneuver. The true error lines are based on ten Monte-Carlo simulations, while the three-sigma line (triple the RSS

Table 2: Values used for each maneuver location.

True Anomaly, θ	Q_{scale}	τ_{scale} (hours)
0°	200	0.35
45°	200	0.35
90°	200	0.65
135°	300	0.75
180°	400	1.00
225°	200	0.65
270°	100	0.50
315°	200	0.35

of the standard deviation of position components) is derived from the EKF time-dependent linear covariance matrix. Since the covariance propagation is linearized, the Monte-Carlo cases were used to validate that approximation. From the data, it is evident that the error reaches a minimum just after periapsis and a maximum just after apoapsis. For the remaining figures in this paper, Monte-Carlo runs are omitted for readability and only three-sigma RSS position errors are considered; however, all linear covariances were validated against a minimum of five Monte-Carlo simulations. After three orbits, the RSS error settles to just under 20 meters 3σ positional.

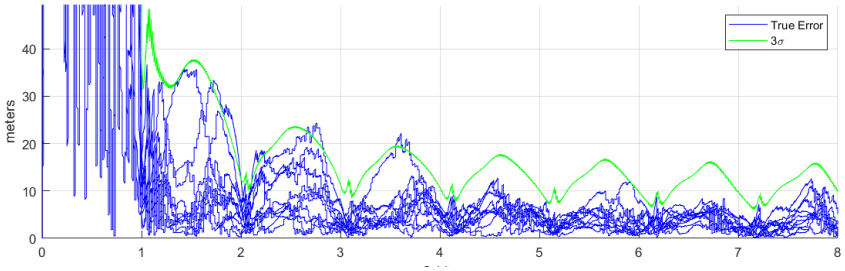

Figure 7: 96-hour simulation of LNN navigation uncertainty (maneuver-free, starting at perilune).

Post-Maneuver Filter Performance

Since the goal of LNN is to provide a PNT service to users, the performance of different maneuver locations is quantified by the percent service availability for four orbits (or 48 hours) after the maneuver is performed. The steady-state performance of 20 meters 3σ is used as the baseline threshold for service in these simulations, since it lies just above the maximum error seen during nominal operations.

Figure 8 shows percent availability for maneuvers being performed at different true anomalies with the filter process noise tuned as given in Table 2. In this plot, performing the maneuver at apoapsis yields the best availability, at 88 percent. However, the worst performing true anomaly is just before at 135°, with an availability of 83 percent. This is a maximum range from best to worst performance across the orbit of just 5%, which is likely within the tolerance of this simulation accuracy and filter tuning.

In fact, filter tuning post-maneuver was found to have a much greater impact on navigation per-

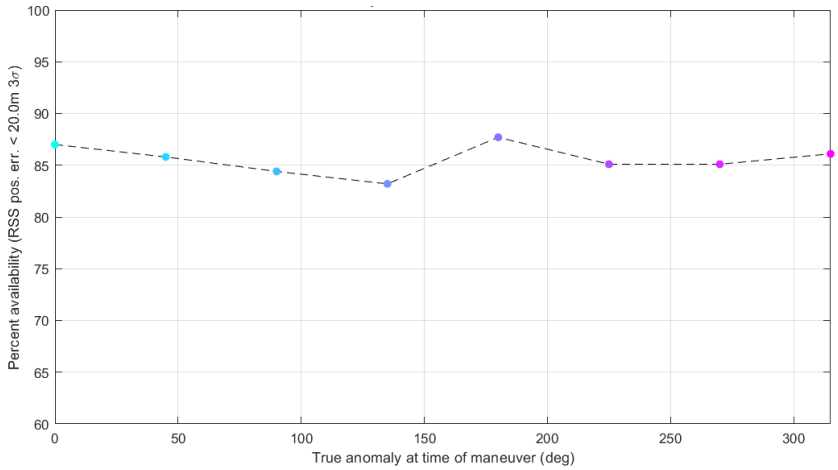

Figure 8: Service availability for four orbits after a maneuver at different true anomalies.

formance than either maneuver direction or location. The tuning parameters for Figure 8 can be found in Table 2 and Figure 9. A very noticeable trend is that the optimum process noise and duration reach a minimum around periapsis and a maximum around apoapsis. This also matches the behavior of filter covariance at the time of the maneuver, suggesting the two may be linked.

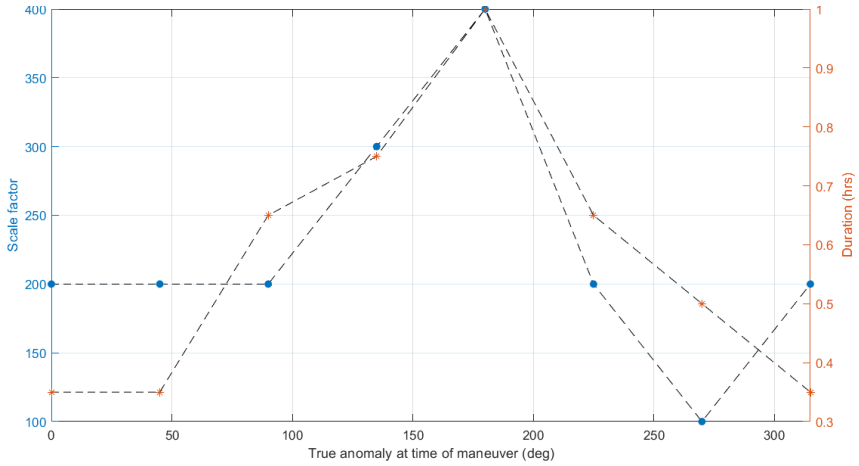

Figure 9: Process noise scale factor and duration post-maneuver for different true anomalies.

To further stress the importance of proper tuning for optimal navigation performance, two separate tunings for the same maneuver are displayed in Figure 10. Here, a 10 cm/s maneuver was performed at the 4th periapsis, and the 3σ RSS error is shown. The first case is poorly tuned, with a scale factor of 500 applied for 2 hours post-maneuver. This case has a much higher peak than the well-tuned variant ($Q_{scale} = 200$ and $\tau = 0.35$ hours), and it takes three orbits to settle down below the 20-meter service threshold. The well-tuned case performs much better – it has an availability for the four orbits post-maneuver of 86.5 percent, compared to just 47.7 percent in the worse-performing case.

One final consideration for navigation is the satellite service volume. Currently, initial LunaNet plans target the lunar South Pole – hence placing apoapsis in the southern hemisphere as opposed

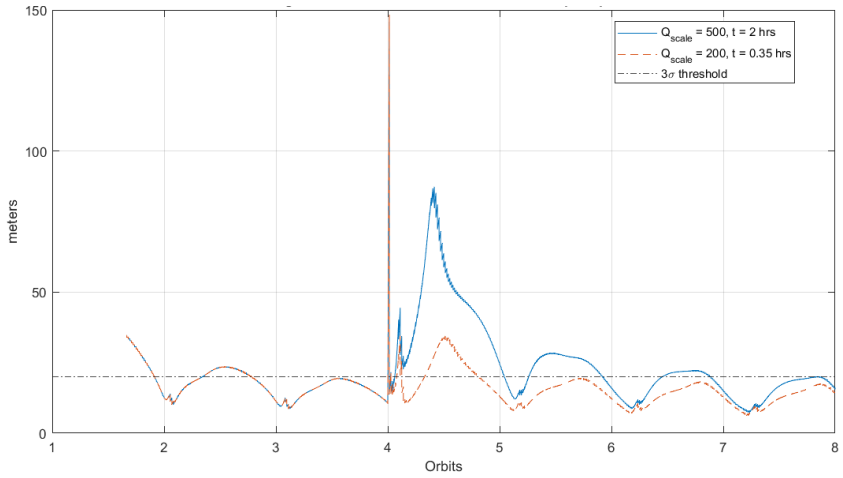

Figure 10: Error for 10 cm/s maneuver at the 4th periapsis with poorly tuned versus well-tuned filters.

to the northern. Ultimately, there will be a defined service volume for LNN, outside of which PNT service is not critical. This will correspond to a range of true anomalies for each orbit, generally centered around the South Pole. Figure 11 shows 3σ errors resulting from maneuvers at different locations, with each simulation starting at the 3rd periapsis; here, the midpoint in the orbit is apoapsis.

With the simulations aligned in this way, it becomes clearer that by performing maneuvers at true anomalies near periapsis (between 270° and 90°), the satellite spends most of its time around apoapsis in violation of the 20-meter OD knowledge requirement for the following orbit. This would mean the satellite could not provide service when most needed, above the South Pole of the Moon. Conversely, performing the maneuver at apoapsis results in a slightly larger error peak, but spends more time in violation of the OD knowledge requirement around periapsis, where the satellite would be outside of the service volume. This provides stronger motivation for using apoapsis as the momentum unloading maneuver location of choice, though future work would be to quantify this once a service volume is solidified.

Orbit Stability at Apoapsis

LunaNet will be providing a critical service for Artemis and human surface users, so service availability will likely be prioritized over orbit stability. As a result, apoapsis is deemed a preferable location over periapsis for momentum unloads based on the two analyses described here. Nevertheless, sending the satellite into an unstable orbit is still undesirable, so orbit stability while performing momentum unloads at apoapsis (rather than periapsis, as shown in Figure 6) was investigated and is shown in Figure 12.

In this simulation, momentum unloads follow the same scheme where they are performed every 14 days and the resultant Δv is directed along the orbit-normal axis – alternating directions each time. Performance is slightly worse than the optimal case since they are being performed at apoapsis rather than periapsis, but the orbit remains stable and follows the trend of the unperturbed case closely.

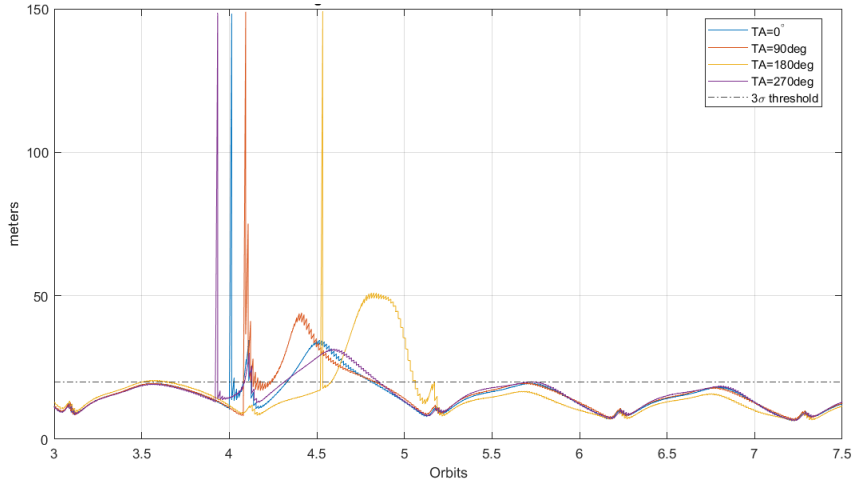

Figure 11: Comparison of 10 cm/s maneuvers at different true anomalies, aligned by orbit position.

CONCLUSION

In this paper, the problem of appropriate placement and direction of momentum unload maneuvers for lunar navigation satellites was considered. A strategy was developed to minimize the negative effect of momentum unloads on position, navigation, and timing service availability and orbit maintenance, based on analysis of long-term orbit propagations and navigation simulations following momentum unloads. For the Lunar Navigation Node (LNN) scenario considered in this paper, performing momentum unloads near apoapsis and in the orbit-normal direction achieves the best service availability while maintaining orbit stability. Adopting this approach will increase service availability of LNN satellites by reducing service outages from momentum unloads, as well as save fuel and extend mission life by minimizing the need for orbit-maintenance maneuvers.

ACKNOWLEDGMENT

Mark Hartigan's work was performed while participating in the Space Communications and Navigation (SCaN) Internship Program through the Office of STEM Engagement at NASA GSFC.

Special thanks to Jose Rosales and Jeff Small in the Navigation and Mission Design branch at GSFC for providing a strong foundation off which this work was based.

REFERENCES

[1] D. J. Israel, K. D. Mauldin, C. J. Roberts, J. W. Mitchell, A. A. Pulkkinen, L. V. D. Cooper, M. A. Johnson, S. D. Christe, and C. J. Gramling, "LunaNet: a Flexible and Extensible Lunar Exploration Communications and Navigation Infrastructure," *2020 IEEE Aerospace Conference*, Big Sky, MT, USA, IEEE, Mar. 2020, pp. 1–14.

[2] D. Israel and N. Babu, "Draft LunaNet Interoperability Specification," July 2022.

[3] J. L. Small, L. M. Mann, J. M. Crenshaw, C. J. Gramling, J. J. Rosales, L. B. Winternitz, M. A. Hassouneh, D. A. Baker, S. Hur-Diaz, and A. J. Liounis, "Lunar Relay Onboard Navigation Performance and Effects on Lander Descent to Surface," Jan. 2022, pp. 587–601. ISSN: 2330-3646.

[4] T. A. Ely, "Stable Constellations of Frozen Elliptical Inclined Lunar Orbits," *The Journal of the Astronautical Sciences*, Vol. 53, Sept. 2005, pp. 301–316.

[5] J. Petersen, "L2 Station Keeping Maneuver Strategy for the James Webb Space Telescope," *Advances in the Astronautical Sciences*, Vol. 171, Portland, ME, american Astronautical Society, Aug. 2019.

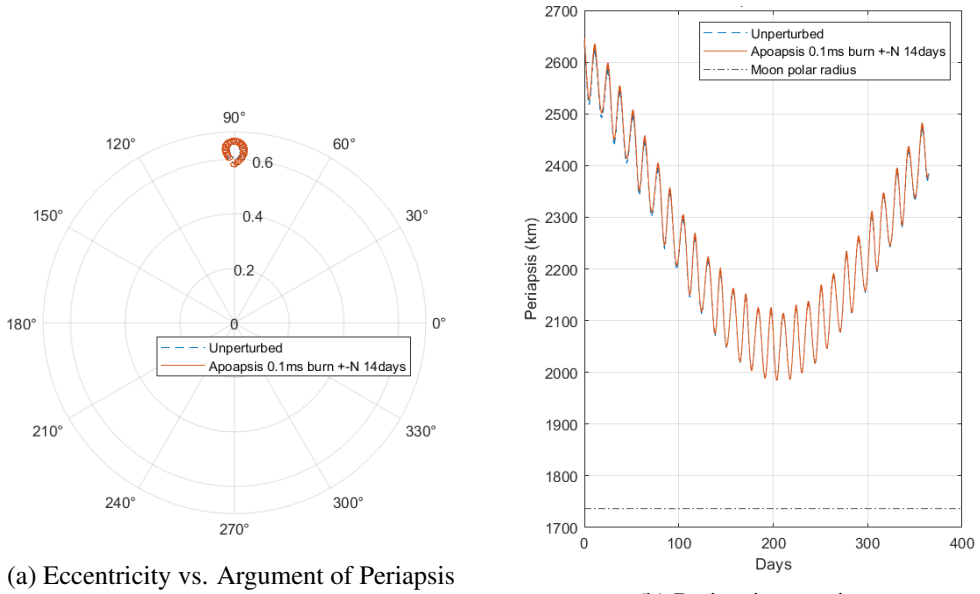

(a) Eccentricity vs. Argument of Periapsis

(b) Periapsis over time

Figure 12: OE over one year with 10 cm/s burns every 14 days along the normal axis at apoapsis, alternating positive and negative directions.

[6] A. Weiss, U. Kalabic, and S. Di Cairano, "Model Predictive Control for simultaneous station keeping and momentum management of low-thrust satellites," *2015 American Control Conference (ACC)*, Chicago, IL, USA, IEEE, July 2015, pp. 2305–2310.

[7] S. Bonasera, N. Bosanac, C. J. Sullivan, I. Elliott, N. Ahmed, and J. W. McMahon, "Designing Sun–Earth L2 Halo Orbit Stationkeeping Maneuvers via Reinforcement Learning," *Journal of Guidance, Control, and Dynamics*, Oct. 2022, pp. 1–11.

[8] P. Silva, H. Lopes, T. Peres, J. Silva, J. Ospina, F. Cichocki, F. Dovis, L. Musumeci, D. Serant, T. Calmettes, I. Pessina, and J. Perelló, "Weak GNSS Signal Navigation to the Moon," *Proceedings of the 26th International Technical Meeting of the Satellite Division of The Institute of Navigation (ION GNSS+ 2013)*, Nashville, TN, Sept. 2013, pp. 3357–3367.

[9] S. Hughes, D. Conway, and J. Parker, "Using the General Mission Analysis Tool (GMAT)," 2017. Publisher: Unpublished.

[10] C. H. Acton, "Ancillary data services of NASA's Navigation and Ancillary Information Facility," *Planetary and Space Science*, Vol. 44, Jan. 1996, pp. 65–70.

[11] C. Acton, N. Bachman, B. Semenov, and E. Wright, "A look towards the future in the handling of space science mission geometry," *Planetary and Space Science*, Vol. 150, Jan. 2018, pp. 9–12.

[12] R. J. Carpenter and C. N. D'Souza, "Navigation Filter Best Practices," Apr. 2018.

[13] J. R. Carpenter, K. Berry, K. Gregory, K. Speckman, S. Hur-Diaz, D. Surka, and D. Gaylor, "Orbit Determination Toolbox," *NASA Tech Briefs, June 2010*, June 2010, pp. 14–15.

[14] P. Zarchan and H. Musoff, *Fundamentals of Kalman filtering: a practical approach*. No. volume 246 in Progress in astronautics and aeronautics, Reston, Virginia: American Institute of Aeronautics and Astronautics, fourth edition ed., 2015.